Inorganica Chimica Acta 362 (2009) 2283–2292

Contents lists available at ScienceDirect

Inorganica Chimica Acta

journal homepage: www.elsevier.com/locate/ica

Control of topology and dimensionality by aromatic dicarboxylate pendant arm position and length in cadmium coordination polymers incorporating a hydrogen-bonding capable kinked dipyridine ligand

Eric Shyu [a], Maxwell A. Braverman [b], Ronald M. Supkowski [c], Robert L. LaDuca [b,*]

[a] *Illinois Mathematics and Science Academy, Aurora, IL 60506, USA*
[b] *Lyman Briggs College and Department of Chemistry, E-30 Holmes Hall, Michigan State University, East Lansing, MI 48825, USA*
[c] *Department of Chemistry and Physics, King's College, Wilkes-Barre, PA 18711, USA*

ARTICLE INFO

Article history:
Received 25 September 2008
Accepted 17 October 2008
Available online 25 October 2008

Keywords:
Cadmium
Coordination polymer
Dicarboxylate
Luminescence

ABSTRACT

Hydrothermal synthesis has afforded three cadmium coordination polymers incorporating both an aromatic dicarboxylate ligand and the kinked and hydrogen-bonding capable organodiimine 4,4′-dipyridylamine (dpa). The positions and length of the pendant arms of the aromatric dicarboxylate moiety exerts a strong structure directing effect in this system. $\{[Cd(hmph)(dpa)] \cdot H_2O\}_n$ (**1**, hmph = homophthalate) possesses interdigitated herringbone (6,3) grid layers with an *ABAB* stacking pattern. $\{[Cd(1,3\text{-phda})(dpa)(H_2O)] \cdot 0.5H_2O\}_n$ (**2**, 1,3-phda = 1,3-phenylenediacetate) exhibits a (4,4)-grid layer structure with two different aperture sizes and an unusual *ABCD* layer stacking pattern. Shortening the pendant arm length resulted in an uncommon $CdSO_4$-type ($6^5 8$ topology) 4-connected 3-D network in $\{[Cd(iph)(dpa)] \cdot 4H_2O\}_n$ (**3**, iph = isophthalate), whose uncoordinated water molecules occupy a sizable incipient void space of 23.7% of the unit cell volume. All three coordination polymers underwent blue-violet luminescence under ultraviolet irradiation.

1. Introduction

The exploratory synthesis and structural analysis of divalent metal dicarboxylate coordination polymers continues to receive significant attention, engendered by the potential industrial applicability of these materials in gas storage [1], molecular separations [2], ion exchange [3], heterogeneous catalysis [4], non-linear optics [5], and luminescence [6]. A tremendous variety of structural morphologies has been observed in these materials, based on the arrangement of the donor groups within the dicarboxylate dianions, their particular binding and bridging modes, and the coordination geometry preferences of the divalent metal ions. Much effort has been extended towards the synthesis of coordination polymers incorporating aromatic dicarboxylate ligands such as isophthalate and terephthalate. Aliphatic α,ω-dicarboxylate ligands have also proven beneficial towards the discovery of new coordination polymer topologies because of their ability to adopt energetically similar conformations during self-assembly [7]. However, coordination polymers constructed from aromatic dicarboxylates tethers with flexible aliphatic pendant arms, such as phenylenediacetate isomers, have been less explored [8].

The structural complexity and functional utility of dicarboxylate-containing inorganic/organic hybrid materials can be enhanced by the incorporation of neutral diimine co-ligands such as the rigid-rod tether 4,4′-bipyridine (4,4′-bpy). These ditopic ligands can connect metal dicarboxylate subunits through the pyridyl nitrogen donor atoms on their periphery, allowing the construction of higher-dimensional solid phases with promising properties [9–11,2]. Several members of this dual-ligand class of coordination polymers with d^{10} ions exhibit luminescent properties [10]. The interpenetrated three-dimensional phase $[Zn(\text{terephthalate})(4,4'\text{-bpy})_{0.5}]$ contains void spaces that permit the chromatographic separation of linear and branched alkanes [2b]. The conformational flexibility of α,ω-dicarboxylate ligands can also facilitate reversible crystal-to-crystal structural rearrangements upon the removal and re-addition of solvent molecules within dual-ligand coordination polymers [12].

Recently we have taken advantage of the kinked donor disposition and the hydrogen bonding capability of 4,4′-dipyridylamine (dpa) to prepare several flexible pendant-arm aromatic dicarboxylate zinc and nickel coordination polymers [13,14]. In these materials and other dpa-containing coordination polymer solids [15–18], the kinked orientation of the dpa nitrogen donor atoms and the hydrogen bonding imparted by the central N–H group tend to act together as structure-directing agents during coordination polymer self-assembly. In the prior zinc [13] and nickel work [14], the coordination environment at the metal was a critical factor in coordination polymer structure. For instance, $[Zn(1,3\text{-phda})(dpa)]_n$ exhibited a chiral 3-D 4-fold interpenetrated diamond lattice

---

* Corresponding author. Tel.: +1 517 432 2268.
E-mail address: laduca@msu.edu (R.L. LaDuca).

0020-1693/$ - see front matter © 2008 Elsevier B.V. All rights reserved.
doi:10.1016/j.ica.2008.10.015

network, but its nickel analogue possessed a simpler non-interpenetrated canted primitive cubic topology. Herein we present the extension of this prior work into a system of cadmium-based pendant-arm aromatic dicarboxylate/dpa coordination polymers, with the synthesis and characterization of $\{[Cd(hmph)(dpa)]\cdot H_2O\}_n$ (**1**, hmph = homophthalate) and $\{[Cd(1,3\text{-}phda)(dpa)(H_2O)]\cdot 0.5H_2O\}_n$ (**2**, 1,3-phda = 1,3-phenylenediacetate). In an effort to explore the effect of restricting conformational flexibility within the pendant arms, $\{[Cd(iph)(dpa)]\cdot 4H_2O\}_n$ (**3**, iph = isophthalate) was also prepared. Compounds **1** and **2** exhibit different two-dimensional covalent connectivities; compound **3** manifests a seldom observed 3-D coordination polymer net. Luminescent and thermal properties are also reported for all three new materials.

2. Experimental section

2.1. General considerations

Cadmium salts were obtained from Fisher, and the dicarboxylic acids were purchased from Aldrich. 4,4′-dipyridylamine (dpa) was prepared via a published procedure [19]. Water was deionized above 3 MΩ in-house. Thermogravimetric analysis was performed on a TA Instruments TGA 2050 Thermogravimetric Analyzer with a heating rate of 10 °C/min up to 900 °C. Elemental Analysis was carried out using a Perkin Elmer 2400 Series II CHNS/O Analyzer. IR spectra were recorded on powdered samples using a Perkin Elmer Spectrum One instrument. Luminescence spectra were obtained with a Hitachi F-4500 Fluorescence Spectrometer on solid crystalline samples anchored to quartz microscope slides with Rexon Corporation RX-22P ultraviolet-transparent epoxy adhesive.

2.2. Preparation of $\{[Cd(hmph)(dpa)]\cdot H_2O\}_n$ (**1**)

$Cd(ClO_4)_2\cdot H_2O$ (100 mg, 0.303 mmol), dpa (110 mg, 0.64 mmol) and homophthalic acid (58 mg, 0.32 mmol), were placed into 10 mL distilled H_2O in a 23 mL Teflon-lined Parr acid digestion bomb. The bomb was sealed and heated at 120 °C for 48 h, whereupon it was cooled slowly to 25 °C. Colorless plates of **1** (119 mg, 0.248 mmol, 82% yield based on Cd) were isolated after washing with distilled water, ethanol, and acetone and drying in air. *Anal.* Calc. for $C_{38}H_{34}Cd_2N_6O_{10}$ **1**: C, 47.57; H, 3.57; N, 8.76. Found: C, 46.72; H, 3.46; N, 8.32%. IR (cm^{-1}): 3385w, 3257w, 3164w, 3059w, 2993w, 1591m, 1546m, 1514s, 1486m, 1440m, 1392s, 1354m, 1342m, 1291w, 1267w, 1207m, 1152w, 1089w, 1056w, 1013s, 960w, 941w, 904w, 853m, 806m, 725m, 693w, 677m, 632m.

2.3. Preparation of $\{[Cd(1,3\text{-}phda)(dpa)(H_2O)]\cdot 0.5H_2O\}_n$ (**2**)

$Cd(ClO_4)_2\cdot H_2O$ (100 mg, 0.303 mmol), dpa (110 mg, 0.64 mmol) and 1,3-phenylenediacetic acid (62 mg, 0.32 mmol), were placed into 10 mL distilled H_2O in a 23 mL Teflon-lined Parr acid digestion bomb. The bomb was sealed and heated at 120 °C for 48 h, whereupon it was cooled slowly to 25 °C. Colorless blocks of **2** (132 mg, 0.271 mmol, 89% yield based on Cd) were isolated after washing with distilled water, ethanol, and acetone and drying in air. *Anal.* Calc. for $C_{20}H_{20}CdN_3O_{5.5}$ **2**: C, 47.77; H, 4.00; N, 8.35. Found: C, 46.97; H, 3.91; N, 8.24%. IR (cm^{-1}): 3166w, 3076w, 2926w, 1592m, 1576m, 1562s, 1520s, 1491m, 1442m, 1393s, 1350s, 1214m, 1152w, 1059m, 1014s, 947w, 906w, 855w, 817s, 757s, 691w, 658s, 634m.

2.4. Preparation of $\{[Cd(iph)(dpa)]\cdot 4H_2O\}_n$ (**3**)

$Cd(NO_3)_2\cdot 4H_2O$ (114 mg, 0.370 mmol), dpa (127 mg, 0.740 mmol) and isophthalic acid (61 mg, 0.37 mmol), were placed into 10 mL distilled H_2O in a 23 mL Teflon-lined Parr acid digestion bomb. The bomb was sealed and heated at 120 °C for 48 h, whereupon it was cooled slowly to 25 °C. Colorless blocks of **3** (146 mg, 0.28 mmol, 76% yield based on Cd) were isolated after washing with distilled water, ethanol, and acetone and drying in air. *Anal.* Calc. for $C_{18}H_{21}CdN_3O_8$ **1**: C, 41.59; H, 4.07; N, 8.08. Found: C, 41.72; H, 3.65; N, 8.20%. IR (cm^{-1}): 3550w br, 2942w, 1596m, 1528s, 1475w, 1444m, 1386s, 1358m, 1217m, 1103w, 1060w, 1016s, 905w, 862w, 835w, 813m, 743s, 718s, 660w.

3. X-ray crystallography

A colourless plate of **1** (with dimensions 0.46 mm × 0.39 mm × 0.10 mm), a colourless block of **2** (0.32 mm × 0.24 mm × 0.14 mm) and a colourless block of **3** (0.40 mm × 0.28 mm × 0.16 mm) were subjected to single crystal X-ray diffraction using a Bruker-AXS SMART 1k CCD instrument. Reflection data were acquired using graphite-monochromated Mo Kα radiation ($\lambda = 0.71073$ Å). The data was integrated via SAINT [20]. Lorentz and polarization effect and empirical absorption corrections were applied with SADABS [21]. The structures were solved using direct methods and refined on F^2 using SHELXTL [22]. All non-hydrogen atoms were refined anisotropically. Hydrogen atoms bound to carbon atoms were placed in calculated positions and refined isotropically with a riding model. The hydrogen atoms bound to the nitrogen atoms of the dpa moieties and any water molecules were found via Fourier difference maps, then restrained at fixed positions and refined isotropically. Relevant crystallographic data for **1**–**3** is listed in Table 1.

4. Results and discussion

4.1. Synthesis and spectral characterization

Compounds **1**–**3** were prepared cleanly as crystalline products by hydrothermal treatment of either cadmium perchlorate (**1** and **2**) or cadmium nitrate (**3**), 4,4′-dipyridylamine, and the requisite dicarboxylic acid. The infrared spectra of **1**–**3** were consistent with their single crystal structures. Sharp, medium intensity bands in the range of ~1600 cm^{-1} to ~1200 cm^{-1} correspond to stretching modes of the aromatic rings of the dpa ligands and dicarboxylate groups [23]. Features corresponding to the puckering of these aromatic rings are observed in the region between 820 cm^{-1} and 600 cm^{-1}. Asymmetric and symmetric C–O stretching modes of the fully deprotonated dicarboxylate anions coincide with the strong broadened bands at ~1590 cm^{-1} and ~1350 cm^{-1}, respectively. The lack of any features in the region of 1700 cm^{-1} indicates the deprotonation of the original dicarboxylic acids. Broadened bands between ~3400 cm^{-1} and ~3200 cm^{-1} in all cases represent N–H stretching modes within the dpa ligands and O–H stretching modes present within the water molecules of crystallization in all complexes.

4.2. Structural description of $\{[Cd(hmph)(dpa)]\cdot H_2O\}_n$ (**1**)

The asymmetric unit of compound **1** contains two cadmium atoms, two hmph dianions (*hmph-A* and *hmph-B*), two dpa ligands (*dpa-A* and *dpa-B*), and two water molecules of crystallization (Fig. 1). Each crystallographically distinct cadmium atoms possesses a $\{CdN_2O_4\}$ coordination geometry, with the *cis* nitrogen donor atoms belonging to two crystallographically distinct dpa ligands. The four remaining coordination sites are occupied by two chelating hmph carboxylate termini: one belonging to a “short” hmph pendant arm and one belonging to a “long” hmph pendant arm. Bond lengths and angles are standard for a chelated octahedral cadmium coordination sphere (Table 2).

Table 1
Crystal and structure refinement data for **1**–**3**.

Data	**1**	**2**	**3**
Empirical formula	$C_{38}H_{34}Cd_2N_6O_{10}$	$C_{20}H_{20}CdN_3O_{5.5}$	$C_{18}H_{21}CdN_3O_8$
Formula weight	959.92	502.79	519.79
Collection *T* (K)	173(2)	173(2)	173(2)
λ (Å)	0.71073	0.71073	0.71073
Crystal system	triclinic	monoclinic	monoclinic
Space group	$P\bar{1}$	$C2/c$	$C2/c$
a (Å)	9.4298(1)	15.924(11)	16.1032(17)
b (Å)	10.3740(1)	23.739(12)	12.5475(13)
c (Å)	19.8803(3)	12.212(8)	20.505(2)
α (°)	85.914(1)	90	90
β (°)	77.183(1)	115.08(6)	100.315(2)
γ (°)	75.246(1)	90	90
V (Å^3)	1833.58(4)	4181(4)	4076.2(7)
Z	2	8	8
D_{calc} (g cm^{-3})	1.738	1.591	1.681
μ (mm^{-1})	1.228	1.083	1.122
Minimum/maximum transmission	0.602/0.888	0.647/0.746	0.743/0.836
hkl Ranges	$-11 \leqslant h \leqslant 11$, $-12 \leqslant k \leqslant 12$, $-23 \leqslant l \leqslant 23$	$-20 \leqslant h \leqslant 20$, $-30 \leqslant k \leqslant 31$, $-15 \leqslant l \leqslant 16$	$-20 \leqslant h \leqslant 20$, $-16 \leqslant k \leqslant 16$, $-26 \leqslant l \leqslant 27$
Total reflections	20212	21868	23968
Unique reflections	6680	4749	4833
R(int)	0.0234	0.0242	0.0246
Parameters/restraints	523/8	281/4	285/7
R_1 (all data)[a]	0.0212	0.0311	0.0420
R_1 ($I > 2\sigma(I)$)[a]	0.0189	0.0249	0.0343
wR_2 (all data)[b]	0.0480	0.0698	0.0755
wR_2 ($I > 2\sigma(I)$)[b]	0.0467	0.0651	0.0724
Maximum/minimum residual (e$^-$/Å^3)	0.351/−0.275	1.170/−0.498	0.787/−0.662
Goodness of fit	1.032	1.053	1.119

[a] $R_1 = \Sigma||F_o| - |F_c||/\Sigma|F_o|$.
[b] $wR_2 = \left\{\sum[w(F_o^2 - F_c^2)^2]/\sum[wF_o^2]^2\right\}^{1/2}$.

Table 2
Selected bond distance (Å) and angle (°) data for **1**.

Cd1–O5	2.2430(13)	N3–Cd1–O6	86.80(5)
Cd1–N3	2.2611(15)	N4–Cd1–O6	148.34(5)
Cd1–N4	2.2975(16)	O3$^{\#1}$–Cd1–O6	92.47(5)
Cd1–O3$^{\#1}$	2.3261(13)	O4$^{\#1}$–Cd1–O6	98.00(5)
Cd1–O4$^{\#1}$	2.3493(14)	N6$^{\#2}$–Cd2–O7	146.64(6)
Cd1–O6	2.5978(15)	N6$^{\#2}$–Cd2–N1	100.24(6)
Cd2–N6$^{\#2}$	2.2681(16)	O7–Cd2–N1	89.58(6)
Cd2–O7	2.2869(15)	N6$^{\#2}$–Cd2–O8	90.84(6)
Cd2–N1	2.2935(16)	O7–Cd2–O8	56.26(5)
Cd2–O8	2.3617(16)	N1–Cd2–O8	113.50(6)
Cd2–O2$^{\#3}$	2.3696(16)	N6$^{\#2}$–Cd2–O2$^{\#3}$	95.13(6)
Cd2–O1$^{\#3}$	2.3798(15)	O7–Cd2–O2$^{\#3}$	97.29(6)
		N1–Cd2–O2$^{\#3}$	140.34(5)
O5–Cd1–N3	111.65(5)	O8–Cd2–O2$^{\#3}$	102.51(6)
O5–Cd1–N4	95.27(5)	N6$^{\#2}$–Cd2–O1$^{\#3}$	98.89(6)
N3–Cd1–N4	103.46(6)	O7–Cd2–O1$^{\#3}$	113.59(5)
O5–Cd1–O3$^{\#1}$	90.59(5)	N1–Cd2–O1$^{\#3}$	86.39(5)
N3–Cd1–O3$^{\#1}$	151.01(5)	O8–Cd2–O1$^{\#3}$	156.03(6)
N4–Cd1–O3$^{\#1}$	92.24(5)	O2–Cd2–O1$^{\#3}$	55.05(5)
O5–Cd1–O4$^{\#1}$	137.25(5)	N4–Cd1–O4$^{\#1}$	110.51(5)
N3–Cd1–O4$^{\#1}$	95.27(5)	O3$^{\#1}$–Cd1–O4$^{\#1}$	56.10(5)
		O5–Cd1–O6	53.40(5)

Symmetry transformation to generate equivalent atoms: (#1) $-x + 1, -y, -z$; (#2) $x + 2, y - 1, z$; (#3) $-x + 3, -y, -z + 1$.

Adjacent Cd1 atoms are bridged by two *hmph-A* ligands in a bis(chelating) binding mode to form [Cd_2(*hmph-A*)$_2$] neutral dinuclear units, in which the Cd···Cd distance is 6.309 Å. Similarly, neighboring Cd2 atoms are conjoined by two *hmph-B* units in a bis(chelating) binding mode to form [Cd_2(*hmph-B*)$_2$] dinuclear kernels, with a Cd···Cd distance is 5.616 Å. Variances in the "short" arm carboxylate torsion angles and in the "long" arm conformations result between the hmph ligands result in the significantly different Cd···Cd distances.

Individual [Cd_2(*hmph-A*)$_2$] and [Cd_2(*hmph-B*)$_2$] dinuclear units are connected by dpa tethering ligands into coordination polymer layers of formulation [Cd(hmph)(dpa)]$_n$, which lie parallel to the (-221) crystal planes (Fig. 2). Again, different Cd···Cd distances are observed because of torsional variances between the crystallographically distinct sets of dpa ligands. A through-ligand Cd···Cd distance of 11.844 Å is provided by *dpa-A*, which has an inter-ring torsion angle equal to 38.1°. On the other hand, *dpa-B* promotes a longer Cd···Cd distance (12.059 Å) possibly because of its slightly more twisted conformation (39.6° inter-ring torsion angle).

Each Cd atom in a [Cd(hmph)(dpa)]$_n$ layer connects to three others: two by means of two different dpa ligands, and one other through two bis(chelating) hmph ligands. Treating the latter

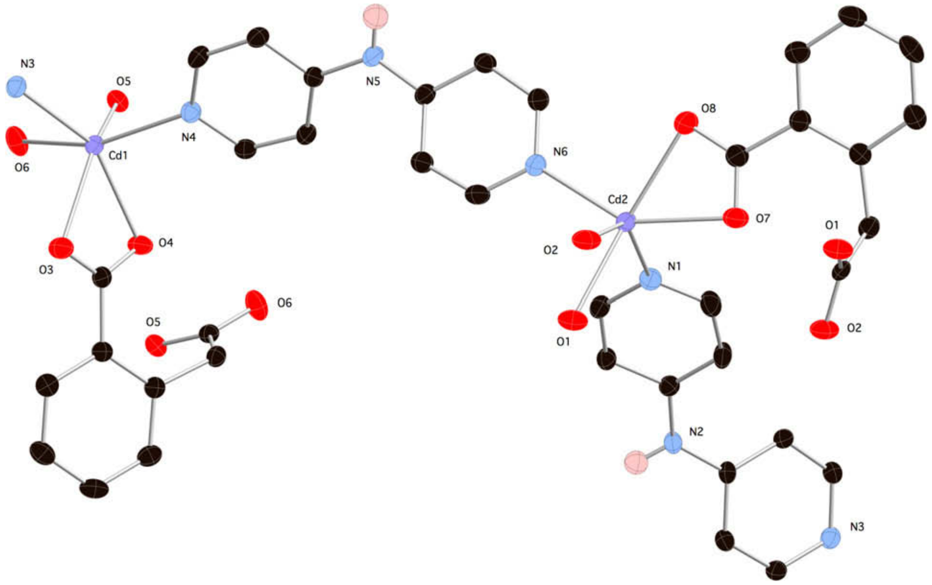

Fig. 1. Coordination environment in **1**, with thermal ellipsoids at 50% probability and atom numbering scheme. Most hydrogen atoms have been omitted for clarity. The water molecules of crystallization are not shown.

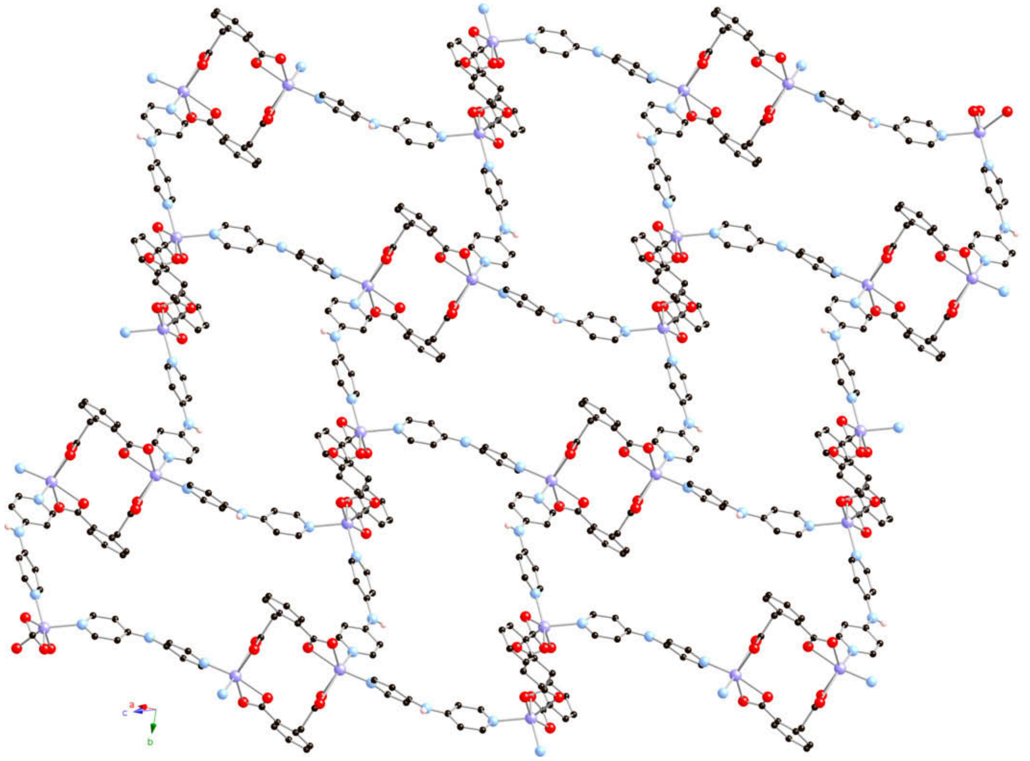

Fig. 2. A single (6,3) herringbone layer motif within **1**, wherein [$Cd_2(hmph)_2$] units are connected by kinked dpa tethers.

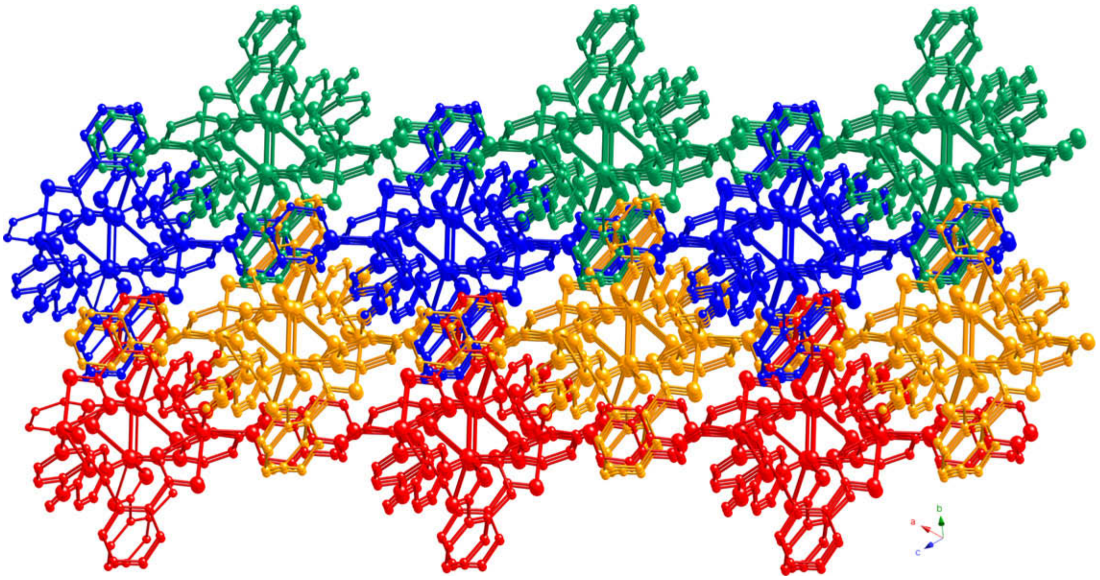

Fig. 3. Interdigitation of four stacked $[Cd(hmph)(dpa)]_n$ coordination polymer layers. The aromatic rings of the hmph ligands in one layer project through pockets formed by kinked dpa ligands in another.

interaction as a single connection allows the layer network in **1** to be considered as a (6,3) "herringbone" type lattice. The [Cd(hmph)(dpa)]$_n$ (6,3) layers interdigitate and stack in an *ABAB* pattern along the *b* crystal direction (Fig. 3), assisted by interlayer hydrogen bonding interactions between dpa amine groups and hmph carboxylate oxygen atoms. Water molecule dimers are located within the small interlamellar regions between the interdigitated layers, which occupy 5.9% of the unit cell volume according to PLATON [24]. Hydrogen bonding data for **1** is given in Table 3.

*4.3. Structural description of {[Cd(1,3-phda)(dpa)(H_2O)] · 0.5H_2O}$_n$ (**2**)*

The asymmetric unit of **2** contains one divalent cadmium ion, one dpa ligand, one bound water molecule, two halves of two crystallographically distinct 1,3-phda ligands (*phda-A*, C11–15/O1–O2; *phda-B*, C21–C25/O3–O4), and one water molecule of crystallization sited on an inversion center (Fig. 4). The cadmium atom is seven-coordinate in a {CdN_2O_5} pentagonal bipyramidal geometry, with the nitrogen atoms in a *trans* orientation belonging to two

Table 3
Hydrogen bonding distance (Å) and angle (°) data for **1**–**3**.

D–H···*A*	*d*(H···*A*)	∠*DHA*	*d*(*D*···*A*)	Symmetry transformation for *A*
Compound ***1***				
O1W–H1WA···O6	1.988(18)	173(3)	2.836(2)	*x*, *y*, *z* + 1
O1W–H1WB···O4	1.937(18)	173(3)	2.803(2)	*x* + 1, *y*, *z* + 1
O2W–H2WA···O1W	1.939(18)	171(3)	2.816(3)	−*x* + 1, −*y* − 1, −*z* + 1
N2–H2N···O5	1.939(18)	162(2)	2.769(2)	*x* + 1, *y*, *z*
N5–H5N···O3	1.963(17)	167(2)	2.791(2)	*x* − 1, *y*, *z*
Compound ***2***				
O1W–H1WA···O1	2.41(7)	123(6)	3.000(3)	
N2–H2N···O4	2.07(3)	171(3)	2.871(3)	−*x* + 1/2, −*y* + 1/2, −*z* + 1
O5–H5A···O3	1.904(18)	173(3)	2.743(3)	−*x*, *y*, −*z* + 3/2
O5–H5B···O2	1.879(18)	169(3)	2.725(3)	−*x* + 1/2, −*y* + 1/2, −*z* + 2
Compound ***3***				
O1W–H1A···O1	1.936(19)	178(4)	2.771(3)	
O1W–H1B···O1W	2.04(2)	164(4)	2.819(6)	−*x*, *y*, −*z* + 1/2
O2W–H2A···O2	2.01(2)	163(4)	2.885(4)	
O2W–H2B···O2	2.13(2)	151(4)	2.961(4)	−*x*, −*y* + 2, −*z*
N2–H2N···O1W	2.05(2)	164(3)	2.902(4)	−*x*, −*y* + 1, −*z*

Table 4
Selected bond distance (Å) and angle (°) data for **2**.

Cd1–N1	2.307(2)	O2–Cd1–O3	163.54(7)
Cd1–O5	2.317(2)	N1–Cd1–O1	91.24(7)
Cd1–N4$^{\#1}$	2.319(2)	O5–Cd1–O1	135.25(8)
Cd1–O2	2.360(3)	N4$^{\#1}$–Cd1–O1	79.11(7)
Cd1–O3	2.385(3)	O2–Cd1–O1	54.02(8)
Cd1–O1	2.513(3)	O3–Cd1–O1	142.29(7)
Cd1–O4	2.536(2)	N1–Cd1–O4	91.78(8)
		O5–Cd1–O4	133.10(7)
N1–Cd1–O5	99.99(7)	N4$^{\#1}$–Cd1–O4	79.37(8)
N1–Cd1–N4$^{\#1}$	166.92(7)	O2–Cd1–O4	143.05(7)
O5–Cd1–N4$^{\#1}$	93.08(7)	O3–Cd1–O4	53.20(8)
N1–Cd1–O2	91.13(8)	O1–Cd1–O4	89.09(9)
O5–Cd1–O2	82.36(8)	O5–Cd1–O3	81.22(8)
N4$^{\#1}$–Cd1–O2	90.30(8)	N4$^{\#1}$–Cd1–O3	91.71(8)
N1–Cd1–O3	90.61(8)		

Symmetry transformation to generate equivalent atoms: (#1) −*x* + 1/2, *y* − 1/2, −*z* + 3/2.

different dpa ligands. The equatorial plane of the coordination sphere is filled by chelating carboxylate termini from two crystallographically distinct 1,3-phda dianions, along with the aqua ligand. Relevant bond lengths and angles for **2** are listed in Table 4.

Each cadmium atom is connected to four others, with one connection through a bis-chelating *phda-A* ligand, one through a bis(chelating) *phda-B* ligand, and two connections *via* dpa tethers which have inter-ring torsion angles of 35.0°. Thus (4,4) grid $[Cd(1,3\text{-phda})(dpa)(H_2O)]_n$ coordination polymer layers are constructed (Fig. 5); these lie parallel to the [1 0 2] crystal planes. The through-ligand Cd···Cd distances are 11.116 Å (through *phda-A*), 12.072 Å (through *phda-B*) and 12.060 Å (through dpa). As can be seen in Fig. 5, two different aperture sizes exist in the $[Cd(1,3\text{-phda})(dpa)(H_2O)]_n$ grid because of the two different 1,3-phda conformations. The smaller apertures measure 7.44 × 8.56 Å, as determined by through-space C···C and N···N distances neglecting van der Waals radii; the aromatic rings of the 1,3-phda ligands point inwards. In comparison the larger apertures (10.80 × 15.22 Å) have the dicarboxylate aromatic rings pointing outwards. Each aperture is surrounded by four apertures of the other type within the $[Cd(1,3\text{-phda})(dpa)(H_2O)]_n$ grid.

The 2-D layer morphology of **2** stands in direct contrast to its nickel analogue $[Ni(1,3\text{-phda})(dpa)(\mu\text{-}H_2O)_{0.5}]_n$, which manifests a non-interpenetrated canted 3-D primitive cubic network topology [14]. In this material, the 1,3-phda ligands link three octahedrally coordinated nickel atoms *via* a monodentate/bis(bridging) mode, connecting $[Ni_2(\mu\text{-}H_2O)_{0.5}]$ dimeric units into a 1-D $[Ni_2(1,3\text{-phda})_2(\mu\text{-}H_2O)_{0.5}]$ chain motif, which in turn are strutted into 3-D by dpa tethers. The differing binding dicarboxylate binding mode and metal coordination geometry in **2** therefore

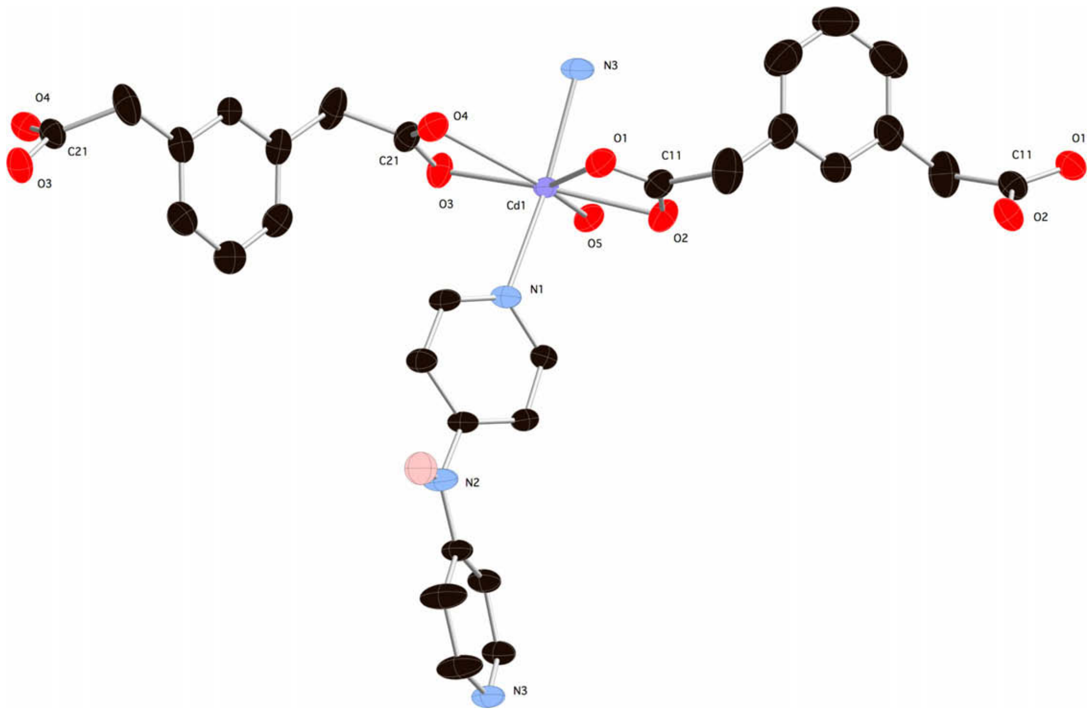

Fig. 4. Coordination environment of **2** with thermal ellipsoids at 50% probability and partial atom numbering scheme. Complete 1,3-phda ligands are shown. Most hydrogen atoms have been omitted for clarity. The water molecule of crystallization is not shown.

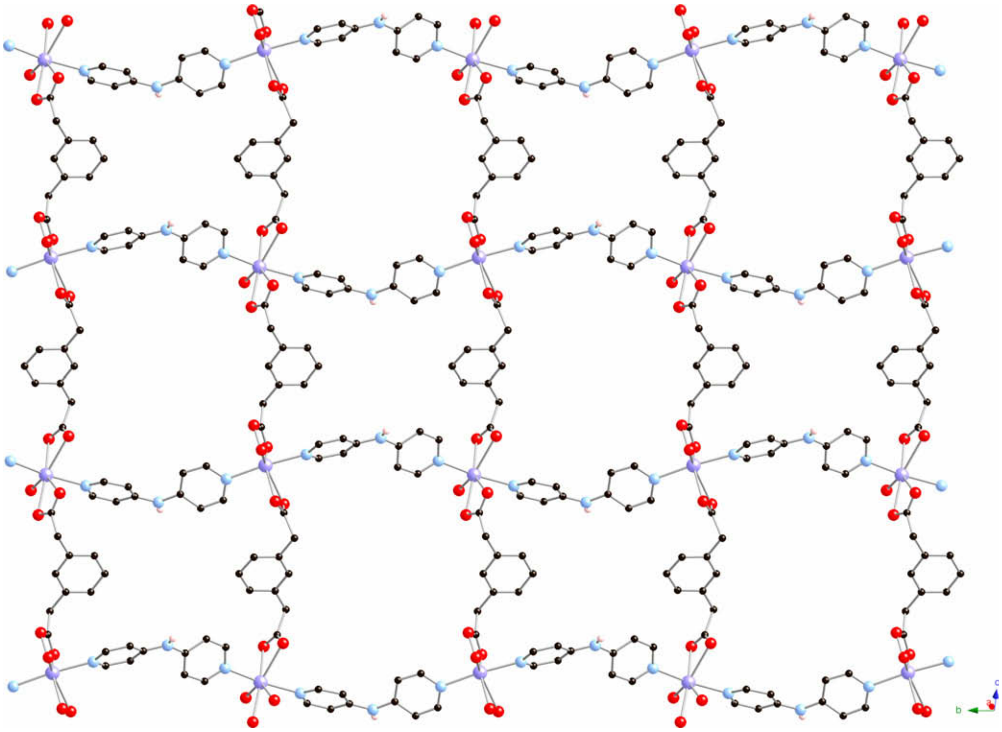

Fig. 5. A single (4,4) grid-like layer pattern in **2**. Two different aperture sizes are evident.

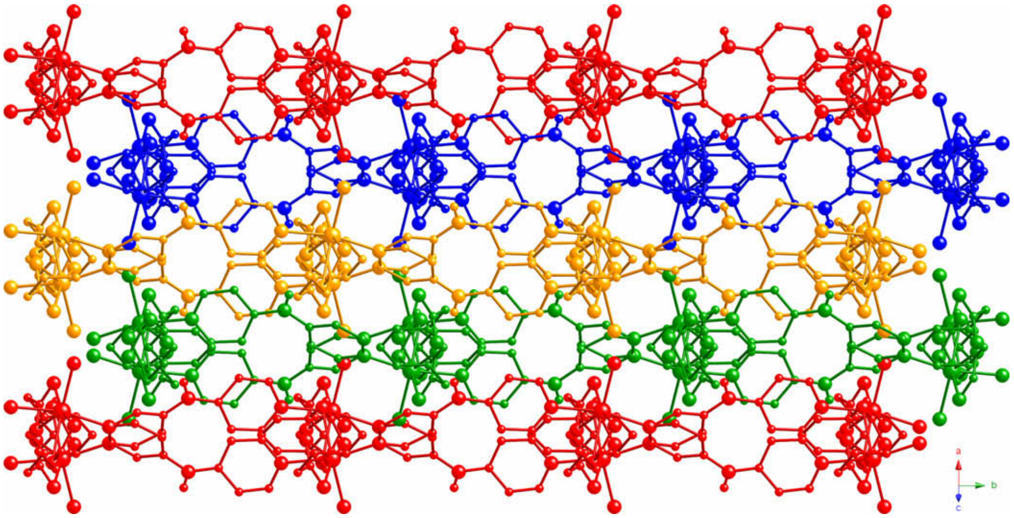

Fig. 6. *ABCD* layer stacking pattern in **2**.

promotes a reduction in coordination polymer dimensionality within this particular system.

Individual $[Cd(1,3\text{-phda})(dpa)(H_2O)]_n$ layers closely stack in a *ABCD* pattern along the *a* crystal direction (Fig. 6), with layer pairs *AB* and *CD* related by crystallographic glide planes and layer pairs *AC* and *BD* related by the crystallographic 2_1 screw axis. The closest Cd···Cd separation between nearest neighboring *A* layers is 15.924 Å, which defines the *a* lattice parameter. Hydrogen bonding interactions between the central amine functional groups of the dpa ligands and aqua ligands, and ligated 1,3-phda carboxylate oxygen atoms provide stability to the stacked layer motif. The water molecules of crystallization are held to the coordination polymer framework through relatively weak hydrogen bonding. Information regarding these supramolecular interactions in **2** is given in Table 3 above. According to PLATON, the unligated water molecules in **2** occupy a scant 3.3% of the overall unit cell volume.

4.4. Structural description of $\{[Cd(iph)(dpa)]\cdot 4H_2O\}_n$ (**3**)

The asymmetric unit of **3** (Fig. 7) is composed of one divalent cadmium atom, one deprotonated iph ligand, a single dpa ligand, and four water molecules of crystallization, one of which is disordered equally over two positions. The coordination environment is best described as a distorted $\{CdN_2O_4\}$ octahedron, with the four oxygen donors belonging to three distinct iph ligands. The *trans*-disposed nitrogen donors belong to two different dpa ligands,

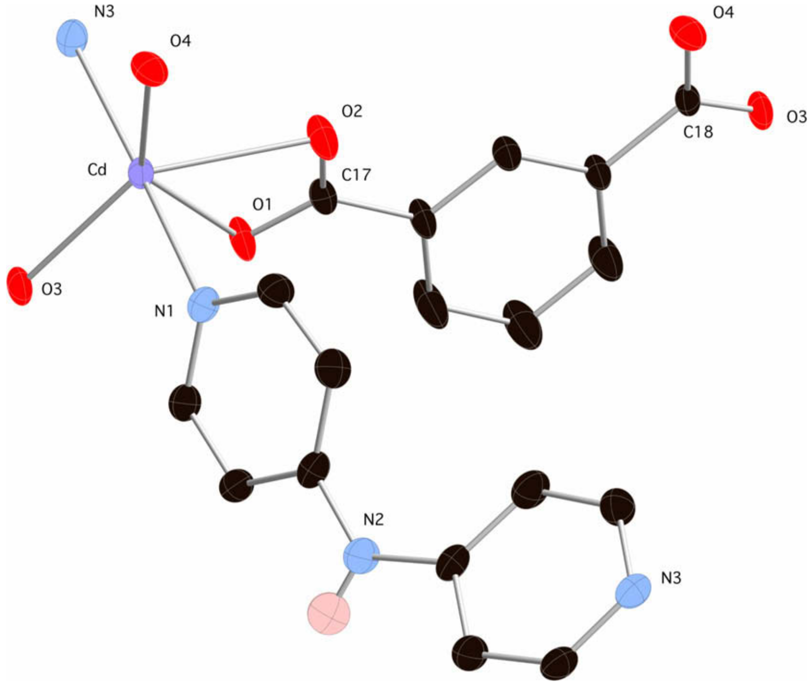

Fig. 7. Coordination environment of **3** with thermal ellipsoids at 50% probability and partial atom numbering scheme. Most hydrogen atoms have been omitted for clarity. The water molecules of crystallization are not shown.

Table 5
Selected bond distance (Å) and angle (°) data for **3**.

Cd1–N3$^{\#1}$	2.266(2)	N3$^{\#1}$–Cd1–O1	96.59(8)
Cd1–N1	2.292(2)	N1–Cd1–O1	88.09(8)
Cd1–O3$^{\#2}$	2.313(2)	O3$^{\#2}$–Cd1–O1	82.59(7)
Cd1–O4$^{\#3}$	2.328(2)	O4$^{\#3}$–Cd1–O1	142.86(7)
Cd1–O1	2.413(2)	N3$^{\#1}$–Cd1–O2	98.66(8)
Cd1–O2	2.440(2)	N1–Cd1–O2	83.90(8)
		O3$^{\#2}$–Cd1–O2	135.84(7)
N3$^{\#1}$–Cd1–N1	175.32(9)	O4$^{\#3}$–Cd1–O2	89.01(7)
N3$^{\#1}$–Cd1–O3$^{\#2}$	92.59(8)	O1–Cd1–O2	53.84(7)
N1–Cd1–O3$^{\#2}$	88.22(8)	N1–Cd1–O4$^{\#3}$	87.82(8)
N3$^{\#1}$–Cd1–O4$^{\#3}$	88.31(8)	O3$^{\#2}$–Cd1–O4$^{\#3}$	134.12(7)

Symmetry transformation to generate equivalent atoms: (#1) $x + 1/2$, $-y + 3/2$, $z + 1/2$; (#2) $x + 1/2$, $y - 1/2$, z; (#3) $-x$, $-y + 2$, $-z$.

which have an inter-ring torsion angle of ~32.3°. Bond lengths and angles are standard for octahedral coordination at divalent cadmium and are given in Table 5. The exotridentate iph anions in **3** display a chelating/bis(bridging) binding mode, with the chelating and bis(bridging) carboxylate termini twisted away from the plane of the iph aromatic ring by ~18° and ~12°, respectively.

Extension of the structure through the iph ligands generates neutral 1-D $[\mathrm{Cd(iph)}]_n$ ribbons constructed from linked $\{\mathrm{CdOCO}\}_2$ 8-membered rings and $\{\mathrm{CdOC_5O}\}_2$ 16-membered ellipsoids (Fig. 8). The through-space Cd···Cd distances across these circuits are 3.79 Å and 7.89 Å, respectively. The $\{\mathrm{CdOCO}\}_2$ units are virtually co-planar, with deviations from planarity ranging only from 0.016 Å to 0.087 Å. Uncoordinated water molecules (O2W) lie above and below the chain, and are hydrogen bonded to oxygen atoms residing within the chelating iph carboxylate termini.

Symmetry-related sets of $[\mathrm{Cd(iph)}]_n$ ribbons are oriented orthogonally with respect to each other, arranged parallel to the *ab* crystal planes. These are linked through tethering dpa ligands, with an inter-chain Cd···Cd distance of 11.85 Å, to construct the covalent 3-D coordination polymer network of **3** (Fig. 9). Hydrogen bonding between the dpa amine groups and iph carboxylate oxygen atoms serves an additional stability-enhancing role (Table 3). Invoking the centroids of the $\{\mathrm{CdOCO}\}_2$ 8-membered rings as connecting nodes, the 3-D coordination polymer network of **3** is an uncommonly encountered 4-connected $\mathrm{CdSO_4}$ lattice ($6^5 8$ topology). Uncoordinated water molecules of crystallization occupy the incipient void spaces within the non-interpenetrated network,

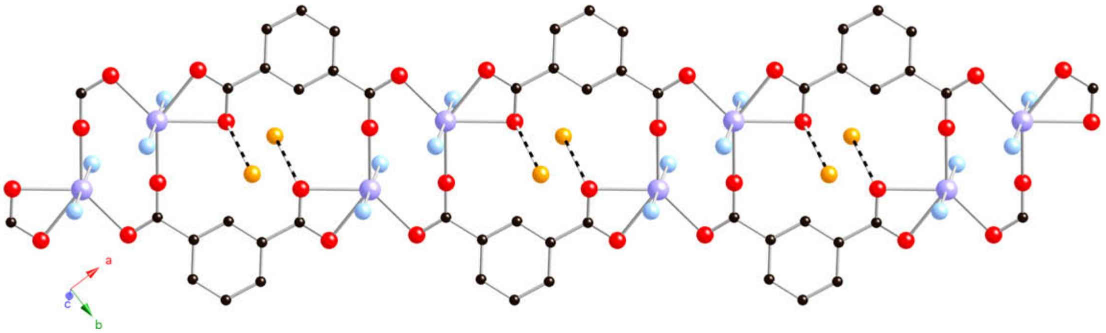

Fig. 8. A single $[\mathrm{Cd(iph)}]_n$ chain in **3**. Hydrogen bonding to water molecules of crystallization entrained within the chain is indicated as dashed lines.

which total 23.7% of the unit cell volume according to PLATON. Although the potential void space in **3** was enticing for gas absorption properties, no measurable N_2 or H_2 absorption was observed despite several attempts with different desolvation and degassing methods.

The 3-D structure of **3** contrasts strongly with other cadmium isophthalate coordination polymers with organodiimine co-ligands. $[Cd(iph)(1,10\text{-phenanthroline})]_n$ and $[Cd(iph)(2,2'\text{-bipyridine})]_n$ are simple 1-D ribbon-like chain polymers [25]. $\{[Cd(iph)(bpmp)] \cdot H_2O\}_n$ (bpmp = bis(4-pyridylmethyl)piperazine) possesses 1-D $[Cd(iph)]_n$ ribbons virtually identical to those in **3** [26]. However, the long quasi-linear reach of the bpmp ligand results in the aggregation of completely parallel sets $[Cd(iph)]_n$ ribbons into a standard (4,4) rectangular grid structure. The kinked donor dispositions of the iph and dpa ligands plausibly act in concert to promote self-assembly of the 3-D 6^58 network of **3**.

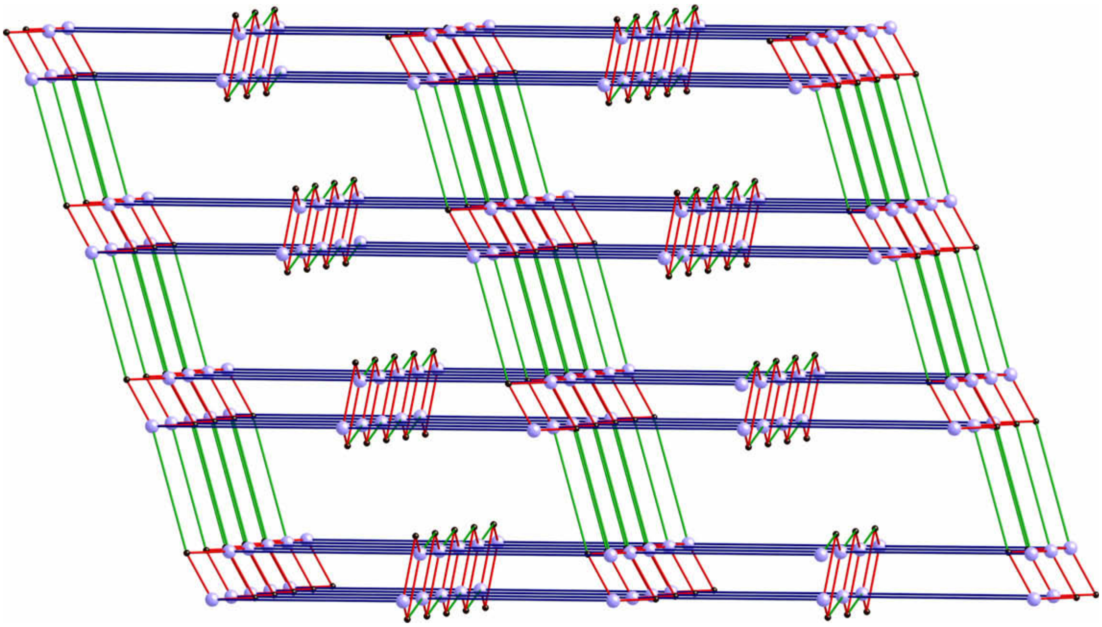

Fig. 9. A view of the 3-D 6^58 topology ($CdSO_4$ structure type) network in **3**.

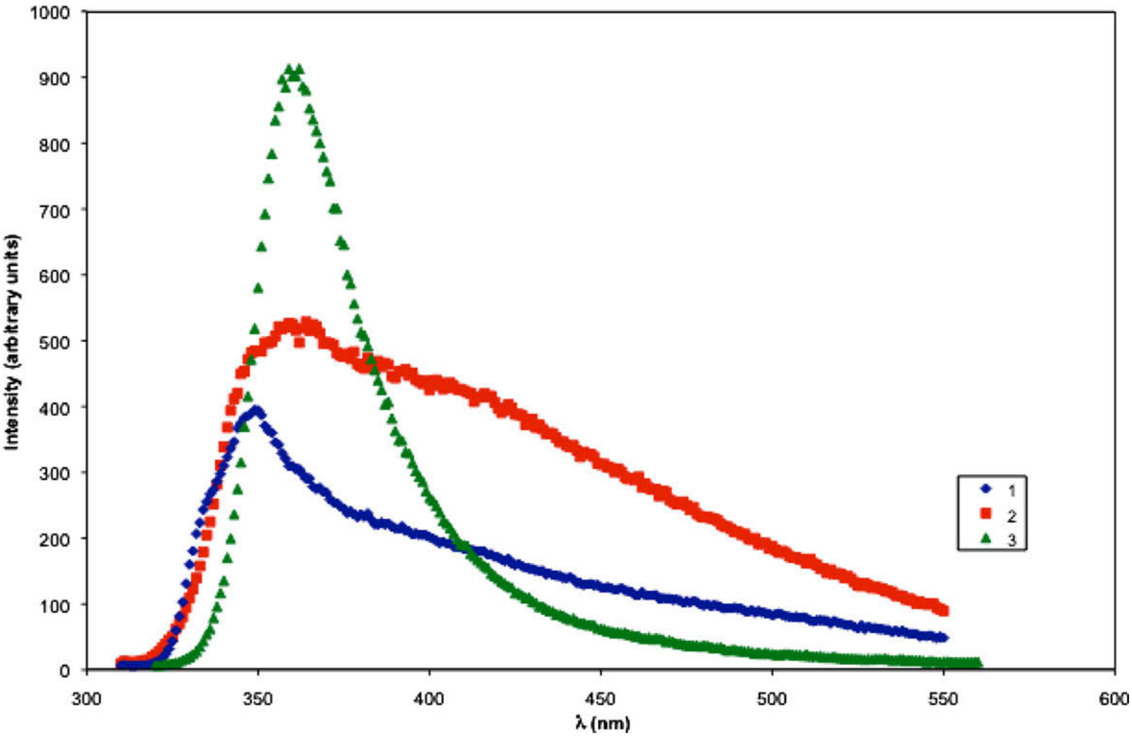

Fig. 10. Emission spectra of **1**–**3**.

4.5. Thermogravimetric analysis

All three coordination polymers were subjected to thermogravimetric analysis under flowing N_2 to probe their dehydration and decomposition behavior. TGA traces for **1**–**3** are shown in Figs. S1–S3. Dehydration of compound **1** occurred slowly between 25 °C and ~150 °C (mass loss 3.7%, calc. for 1 equiv. of water 3.8%). Removal of the organic components occurred between ~280 °C and ~600 °C, with a mass loss of 69.4% roughly corresponding to the ejection of the dpa and hmph ligands (72.8% calc.). The mass remnant of 26.3% at ~600 °C matches well for the deposition of CdO (25.0% predicted).

Compound **2** also underwent slow dehydration from 25 °C to ~220 °C, with a 6.2% mass loss that is roughly consistent with the ejection of the water molecules (5.4% predicted). Removal of the organic components occurred between ~220 °C and ~640 °C. The mass remnant at ~640 °C is 31.0%, indicating a mixture of CdO (22.0% predicted) and uncombusted organics. Compound **3** underwent dehydration between 25 °C and ~65 °C, with a mass loss roughly corresponding to loss of two water molecules of crystallization (6.0% mass loss observed, 7.2% predicted). It is likely that some of the co-crystallized water had left the sample upon standing. Ejection of the organic components occurred between ~370 °C and ~650 °C, as marked by a series of mass losses totaling 66% of the original mass, corresponding to the expulsion of one equivalent of both iph and dpa ligands (66.8% predicted). The 26.7% mass remnant at 650 °C matches well with the deposition of CdO (25.5% predicted).

4.6. Luminescent behavior of **1–3**

Irradiation of complexes **1–3** with ultraviolet light ($\lambda = 300$ nm) in the solid state resulted in blue-violet visible light emission in all cases (Fig. 10). As in other cadmium-based coordination polymers [27], the emissive behavior is plausibly ascribed to ligand-centered $\pi-\pi$ electronic transitions within the molecular orbital systems of the aromatic dicarboxylate and/or the dpa ligands. The breadth of the emission features for **1** and **2** is attributed to intensity diminishing vibrational modes provided by the flexible pendant arms of the hmph or 1,3-phda ligands. The greater rigidity of the iph ligands in **3** could potentially minimize radiative energy loss pathways, resulting in a narrower and more intense luminescence spectral profile.

5. Conclusions

Changing the pendant arm length and orientation within aromatic dicarboxylates has permitted the synthesis of luminescent 2D and 3D cadmium coordination polymers incorporating the kinked and hydrogen-bonding donating dpa co-ligand. The wider-spanning 1,3-phda ligand, with its *meta* disposition of acetate groups, resulted in a (4,4) grid structure in **2** in which noticeably different grid apertures are induced by the conformational flexibility of the ligand pendant arms. Shortening one of the pendant arms and shifting to an *ortho* carboxylate disposition in the hmph ligand did not alter the coordination polymer dimensionality. However, the layer topology was adjusted into a herringbone pattern in the case of **1**. The use of an *meta* substituted aromatic dicarboxylate with rigid arms resulted in a 3-D coordination polymer with an uncommon topology in **3**. The flexible coordination geometry at cadmium, because of its lack of crystal field stabilization, can adapt to the steric and geometric requirements of both dicarboxylate and diimine donors in this system. In **1**–**3**, hydrogen-bonding donation provided by the central amine of the dpa ligand plays a significant auxiliary structure-directing role. Further synthetic explorations towards dpa-based divalent metal carboxylate coordination polymers are underway in our laboratory.

Acknowledgments

Funding for this work was provided by Michigan State University and the donors of the American Chemical Society Petroleum Research Fund. E.S. thanks the MSU High School Honors Science Program and Dr. Gail Richmond for his participation in the research. We thank Dr. Rui Huang for performing the elemental analyses and Dr. Kathryn Severin for use of the fluorimeter. We also thank Dr. Wayne Ouellette of Syracuse University for the gas absorption studies.

Appendix A. Supplementary material

Supplementary data associated with this article can be found, in the online version, at doi:10.1016/j.ica.2008.10.015.

References

[1] (a) H. Li, M. Eddaoudi, M. O'Keeffe, O.M. Yaghi, Nature 402 (1999) 276;
(b) R. Matsuda, R. Kitaura, S. Kitagawa, Y. Kubota, R.U. Belosludov, T.C. Kobayashi, H. Sakamoto, T. Chiba, M. Takata, Y. Kawazoe, Y. Mita, Nature 436 (2005) 238;
(c) L. Pan, D. Holson, L.R. Ciemnolonski, R. Heddy, J. Li, Angew. Chem., Int. Ed. 45 (2006) 616;
(d) N.L. Rosi, J. Eckert, M. Eddaoudi, D.J. Vodak, J. Kim, M. O'Keeffe, O.M. Yaghi, Science 300 (2003) 1127;
(e) M. Dinca, A.F. Yu, J.R. Long, J. Am. Chem. Soc. 128 (2006) 8904;
(f) G. Ferey, M. Latroche, C. Serre, F. Millange, T. Loiseau, A. Percheron-Guegan, Chem. Commun. (2003) 2976;
(g) X. Zhao, B. Xiao, A.J. Fletcher, K.M. Thomas, D. Bradshaw, M.J. Rosseinsky, Science 306 (2004) 1012.

[2] (a) J.S. Seo, D. Whang, H. Lee, S.I. Jun, J. Oh, Y.J. Jeon, K. Kim, Nature 404 (2000) 982;
(b) B. Chen, C. Liang, J. Yang, D.S. Contreras, Y.L. Clancy, E.B. Lobkovsky, O.M. Yaghi, S. Dai, Angew. Chem., Int. Ed. 45 (2006) 1390;
(c) O.M. Yaghi, H. Li, T.L. Groy, J. Am. Chem. Soc. 118 (1996) 9096;
(d) O.M. Yaghi, C.E. Davis, G. Li, H. Li, J. Am. Chem. Soc. 119 (1997) 2861.

[3] (a) Q.-R. Fang, G.-S. Zhu, M. Xue, J.-Y. Sun, S.-L. Qiu, Dalton Trans. (2006) 2399;
(b) X.-M. Zhang, M.-L. Tong, H.K. Lee, X.-M. Chen, J. Solid State Chem. 160 (2001) 118;
(c) O.M. Yaghi, H. Li, T.L. Groy, Inorg. Chem. 36 (1997) 4292.

[4] (a) N. Guillou, P.M. Forster, Q. Gao, J.S. Chang, M. Nogues, S.-E. Park, A.K. Cheetham, G. Ferey, Angew. Chem., Int. Ed. 40 (2001) 2831;
(b) C.-D. Wu, A. Hu, L. Zhang, W. Lin, J. Am. Chem. Soc. 127 (2005) 8940;
(c) H. Han, S. Zhang, H. Hou, Y. Fan, Y. Zhu, Eur. J. Inorg. Chem. (2006) 1594;
(d) W. Mori, S. Takamizawa, C.N. Kato, T. Ohmura, T. Sato, Micropor. Mesopor. Mater. 73 (2004) 15.

[5] (a) S. Zang, Y. Su, Y. Li, Z. Ni, Q. Meng, Inorg. Chem. 45 (2006) 174;
(b) L. Wang, M. Yang, G. Li, Z. Shi, S. Feng, Inorg. Chem. 45 (2006) 2474;
(c) S. Wang, Y. Hou, E. Wang, Y. Li, L. Xu, J. Peng, S. Liu, C. Hu, New J. Chem. 27 (2003) 1144.

[6] (a) L.G. Beauvais, M.P. Shores, J.R. Long, J. Am. Chem. Soc. 122 (2000) 2763;
(b) H. Jianghua, Y. Jihong, Z. Yuetao, P. Qinhe, X. Ruren, Inorg. Chem. 44 (2005) 9279.

[7] (a) D. Ghoshal, A.K. Ghosh, G. Mostafa, J. Ribas, N.R. Chaudhuri, Inorg. Chim. Acta 360 (2007) 1771;
(b) C. Livage, C. Egger, M. Nogues, G. Ferey, Compt. Rend. Acad. Sci. Ser. Chem. 4 (2001) 221.

[8] (a) L. Pan, K.M. Adams, H.E. Hernandez, X. Wang, C. Zheng, Y. Hattari, K. Kaneko, J. Am. Chem. Soc. 125 (2003) 3062;
(b) Y.-F. Zhou, R.-H. Wang, B.-L. Wu, R. Cao, M.-L. Hong, J. Mol. Struct. 697 (2004) 73;
(c) J. Zhou, C. Sun, J. Linpei, J. Mol. Struct. 832 (2007) 55;
(d) Y. Yang, M.-H. Zheng, S.H. Zhang, H. Liang, Acta Crystallogr. E63 (2007) m2392.

[9] (a) W.-G. Lu, C.-Y. Su, T.-B. Lu, L. Jiang, J.-M. Chen, J. Am. Chem. Soc. 128 (2006) 34;
(b) S. Horike, R. Matsuda, S. Kitagawa, Stud. Surf. Sci. Catal. 156 (2005) 725;
(c) C. Qin, X.-L. Wang, Y.-G. Li, E.-B. Wang, Z.-M. Su, L. Xu, R. Clerac, Dalton Trans. (2005) 2609;
(d) Y.-Q. Zheng, E.-R. Ying, Polyhedron 24 (2005) 397;
(e) S.K. Ghosh, J. Ribas, P.K. Bharadwaj, Cryst. Growth Des. 5 (2005) 623;
(f) X.-Z. Sun, Y.-F. Sun, B.-H. Ye, X.-M. Chen, Inorg. Chem. Commun. 6 (2003) 1412.

[10] L. Xu, G.-C. Guo, B. Liu, M.-S. Wang, J.-S. Huang, Inorg. Chem. Commun. 7 (2004) 1145.
[11] H.-P. Jia, W. Li, Z.-F. Ju, J. Zhang, Eur. J. Inorg. Chem. (2006) 4264.
[12] M.R. Montney, S. Mallika Krishnan, R.M. Supkowski, R.L. LaDuca, Inorg. Chem. 46 (2007) 7362.
[13] M.A. Braverman, R.L. LaDuca, Cryst. Growth Des. 7 (2007) 2343.
[14] M.A. Braverman, R.J. Staples, R.M. Supkowski, R.L. LaDuca, Polyhedron 27 (2008) 2291.
[15] M.A. Braverman, R.M. Supkowski, R.L. LaDuca, J. Solid State Chem. 180 (2007) 1852.
[16] M.A. Braverman, R.M. Supkowski, R.L. LaDuca, Inorg. Chim. Acta 360 (2007) 2353.
[17] D.P. Martin, R.M. Supkowski, R.L. LaDuca, Inorg. Chem. 46 (2007) 7917.
[18] K.A. Brown, D.P. Martin, R.M. Supkowski, R.L. LaDuca, CrystEngCommun 10 (2008) 846.
[19] P.J. Zapf, R.L. LaDuca, R.S. Rarig, K.M. Johnson, J. Zubieta, Inorg. Chem. 37 (1998) 3411.
[20] SAINT, Software for Data Extraction and Reduction, Version 6.02 Bruker AXS, Inc., Madison, WI, 2002.
[21] SADABS, Software for Empirical Absorption Correction, Version 2.03 Bruker AXS, Inc., Madison, WI, 2002.
[22] G.M. Sheldrick, SHELXTL, Program for Crystal Structure Refinement, University of Göttingen, Göttingen, Germany, 1997.
[23] M. Kurmoo, C. Estournes, Y. Oka, H. Kumagai, K. Inoue, Inorg. Chem. 44 (2005) 217.
[24] A.L. Spek, PLATON A Multipurpose Crystallographic Tool, Utrecht University, Utrecht, The Netherlands, 1998.
[25] A. Thirumurugan, C.N.R. Rao, J. Mater. Chem. 15 (2005) 3852.
[26] D.P. Martin, M.A. Braverman, R.L. LaDuca, Cryst. Growth Des. 7 (2007) 2609.
[27] (a) J. Tao, J.X. Shi, M.L. Tong, X.X. Zhang, X.M. Chen, Inorg. Chem. 40 (2001) 6328;
(b) J. Tao, M.L. Tong, J.X. Shi, X.M. Chen, S.W. Ng, Chem. Commun. (2000) 2043;
(c) J.C. Dai, X.T. Wu, Z.Y. Fu, C.P. Cui, S.M. Hu, W.X. Du, L.M. Wu, H.H. Zhang, R.Q. Sun, Inorg. Chem. 41 (2002) 1391;
(d) W. Chen, J.Y. Wang, C. Chen, Q. Yue, H.M. Yuan, J.S. Chen, S.N. Wang, Inorg. Chem. 42 (2003) 944;
(e) N. Hao, E. Shen, Y.B. Li, E.B. Wang, C.W. Hu, L. Xu, Eur. J. Inorg. Chem. (2004) 4102.